land

MDPI

Article

A Simulation-Based Study on the Impact of Parametric Design on Outdoor Thermal Comfort and Urban Overheating

Cheuk Yin Wai [1,2,*], Muhammad Atiq Ur Rehman Tariq [3], Hing-Wah Chau [1,2], Nitin Muttil [2] and Elmira Jamei [1,2,*]

[1] College of Sport, Health and Engineering, Victoria University, P.O. Box 14428, Melbourne, VIC 8001, Australia; hing-wah.chau@vu.edu.au
[2] Institute for Sustainable Industries and Liveable Cities, Victoria University, P.O. Box 14428, Melbourne, VIC 8001, Australia; nitin.muttil@vu.edu.au
[3] Centre of Excellence in Water Resources Engineering, G.T. Road, Lahore 54890, Pakistan; atiq.tariq@cewre.edu.pk
* Correspondence: cheuk.wai@live.vu.edu.au (C.Y.W.); elmira.jamei@vu.edu.au (E.J.)

Abstract: Under the current energy crisis and climate change, sustainable urban planning and building design are a priority to achieve a net-zero future, as energy use in buildings for thermal comfort is one of the major carbon emission contributors. To adapt to a rapidly growing and stringent urban environment, where buildings are causing more emissions due to more frequent and severe extreme hot weather events, the parametric design approach has great potential and flexibility in providing a sustainable solution by simulating different design scenarios. This study aims to analyse urban geometry and identify the impact of various built environment scenarios on outdoor thermal comfort under certain climates. The Grasshopper program was used along with the Ladybugs plug-in to provide visualised outcomes of outdoor thermal comfort, with simulation models on Rhinoceros 3D Version 7 SR37 (7.37.24107.1500). Comparing the thermal comfort performance of different design scenarios, based on building height, orientation and urban geometry, helps to identify which factors are more impactful on building design. This study demonstrates the workflow of parametric design in analysing the microclimate pattern and outdoor thermal comfort performance of the existing built environment in Melbourne, Australia, to provide an insight for stakeholders and builders to inform better decision-making in urban planning and building design in order to achieve a zero-emission future.

Keywords: urban heat; thermal comfort; urban geometry; built environment; heatwave; passive cooling; parametric design; generative algorithms; Rhinoceros 3D; Grasshopper plug-in

Citation: Wai, C.Y.; Tariq, M.A.U.R.; Chau, H.-W.; Muttil, N.; Jamei, E. A Simulation-Based Study on the Impact of Parametric Design on Outdoor Thermal Comfort and Urban Overheating. *Land* **2024**, *13*, 829. https://doi.org/10.3390/land13060829

Academic Editors: Giuseppe T. Cirella and Alessio Russo

Received: 6 May 2024
Revised: 2 June 2024
Accepted: 4 June 2024
Published: 10 June 2024

1. Introduction

With the rapid growth of population and increase in urban areas around the world, more urban dwellers are experiencing risks prompted by the urban heat island (UHI) effects combined with extreme hot weather events. UHI effects occur when the built-up environment contains higher temperatures compared with the surrounding suburbs or rural areas [1]. One of the causative factors is that the built-up areas are covered by building materials with higher heat absorption than the suburban or rural areas with a higher ratio of vegetation coverage or of water bodies [2,3]. Another factor that causes the UHI effect is the urban geometry formed by high-rise buildings that alter the air dynamics in between street canyons, which potentially prevents cool prevailing winds from entering the core of the city and limits natural ventilation for cooling [4]. Many studies have mentioned the potential risks that urban heat poses to human health and well-being, which can be fatal under extremely hot weather events [5,6]. To overcome the issues of increased urban heat situations, most urban dwellers excessively rely on the use of HVAC systems, which, however, increases energy consumption and greenhouse gas emissions in the long term.

Heating and cooling in buildings is one of the most energy-consuming factors globally. According to the International Energy Agency (IEA), heat is the largest energy end-use, accounting for 50% of global final energy consumption in 2018, with 46% of total heat produced consumed in buildings for space heating and cooling [7]. Similar records observed in Australia demonstrate that about 40% of the energy used in the average Australian household is for heating and cooling [8]. With the impacts of climate change, there is an increase in energy consumption in buildings for heating and cooling to maintain human thermal comfort. According to the Department of Climate Change, Energy, the Environment and Water (DCCEEW) (2023), there was a 3% rise in energy consumption in the residential sector and in the commercial and services sector between 2021 and 22, due to the warmer summer and cooler winter compared to the previous year [9]. However, electricity and heat are also the largest contributors to annual greenhouse gas emissions, with 15.18 billion tonnes of carbon dioxide emission recorded in 2020 [10]. As a result, the extensive use of HVAC systems for heating or cooling will eventually re-contribute to the climate change process, hence introducing more frequent and severe extreme weather events in the future.

Therefore, it is necessary to explore other potential UHI mitigation strategies, which can prevent the vicious cycle between climate change and energy consumption in the long term. One of the main UHI mitigation strategies is urban geometry manipulation to create shading effects by arranging buildings and trees strategically, which provides the greatest potential for comfort enhancement at the neighbourhood scale [11,12]. To analyse the urban heat island effect at this neighbourhood level, simulation tools are commonly used due to their capability to provide spatial analysis, and the feasibility of adjusting the study parameters based on the climate zone of the study area, scale of investigation, and availability of local data collections [13]. However, as mentioned by Kim and Brown, there are no extensively investigated attempts to analyse the daily UHI fluctuations with three-dimensional interpretation of the city energy budget based on urban geometry, and at a small scale only [14]. This might be because each piece of simulation software has different strengths and limitations. A typical challenge in city-scale simulation is the time-consuming calculation process, which also correlates to the requirements of the computer hardware [15]. Due to this limited study of UHI and urban thermal behaviour using 3D spatial analysis at a neighbourhood scale, there is a need to identify a feasible evaluation method by comparing different simulation tools and indicators for such context. Therefore, the aim of this study is to establish a comprehensive workflow using simulation software integrated with parametric design approaches for early-stage design, which provide significant insights for urban planners, architects, and stakeholders, to create different scenarios and access how the change in built environments can impact the microclimate pattern and outdoor thermal comfort at neighbourhood scale. Furthermore, this study will contribute to showcase the practical use of the parametric design principle in urban climate research with controllable and adaptable outcomes.

2. Literature Review

Numerous indicators and methods have been used for analysing urban heat and outdoor thermal comfort. One of the most popular methods used by other studies is calculating the UHI intensity by comparing the difference in atmospheric air temperature (Tair) or the land surface temperature (LST) between urban areas and rural areas [14,16–19]. However, these methods rely on using meteorological data collected from local weather stations or measuring instruments on site, which means that the data may not be sufficient to provide an overview of the spatial distribution across the city [20,21]. The other common method to analyse UHI is using remote sensors from satellites to generate satellite images and then process these with any Geographic Information System (GIS) software to obtain spatial data; this method is capable of covering a large amount of area which makes it popular in city-scale studies [22,23]. The limitation of this method is that the coverage of satellite images might not always be available due to weather conditions or the operation orbits of the satellites, and the results may vary due to the defined urban area and the

selected factors [24]. Therefore, numerical simulation methods are the most reliable for conducting mesoscale urban heat island analysis [25]. Although urban heat analysis allows us to understand the thermal behaviour of the physical environment, these urban heat indicators do not necessarily represent the physiological aspect of the human body's feelings towards its surroundings [26]. Hence, human thermal comfort indexes are introduced to provide a better interpretation from a human physiological perspective under the different microclimate conditions caused by urban heat.

2.1. Human Thermal Comfort Indexes

Similar to the urban heat indicators, a wide range of indexes have been used to evaluate human thermal comfort, such as the Predicted Mean Vote (PMV), Thermal Sensation Votes (TSVs). Physiological Equivalent Temperature (PET), Universal Thermal Climate Index (UTCI), Predicted Percent of Dissatisfied People (PPD), Index of Thermal Stress (ITS), Perceived temperature (PT), Operative Temperature (OP), Mean Radiant Temperature (MRT), Net Effective Temperature (NET), and Standard Effective Temperature (SET) [27–30].

One of the most commonly used thermal comfort indexes is the Predicted Mean Vote (PMV). It was developed by Fanger [31] and takes into consideration human perception of the thermal environment. It has been standardized in ISO 7730 [32] and can be associated with the seven-point thermal sensation scale under the ASHRAE standard 55 [32]. Based on Fanger's PMV model, the Pierce and KSU models were implemented to predict thermal sensation based on a different physiological model. The Pierce model can be referred to as the PMV Effective Temperature, and the KSU model is known as Thermal Sensational Vote (TSV) [33]. These two models use a nine-point sensation scale instead. As mentioned by [34], the static PMV model performs better in the controlled environment of an indoor space instead of in an open area or space with natural ventilation.

Another commonly used index is the Universal Thermal Climate Index (UTCI). The UTCI is a measure of the human physiological response to the thermal environment, in terms of the heat exchanges between a human body and the thermal environment [35]. The UTCI is calculated by using air temperature, relative humidity, wind speed and mean radiant temperature [36]. The UTCI can also divided into 10 thermal stress categories that correspond to specific human physiological responses to the thermal environment [37]. A relatively new index is the Physiological Equivalent Temperature (PET), which uses the Munich Energy-balance Model for Individuals (MEMI), which analysed the thermal conditions of the human body in a physiologically relevant way [38]. Similar to the PMV and UTCI, PET can be rated in different grades of thermal precipitation and physiological stress [39,40]. Table 1 below provides a brief overview of different thermal comfort indexes scales accordingly.

Table 1. Comparison of different thermal comfort indexes: UTCI, Fanger's PMV, TSV, and PET.

UTCI Thermal Stress Categories		**Fanger's PMV Seven-Point Scale**		**Thermal Sensation Vote**		**PET Grade of Physiological Stress**	
Above +46 °C	Extreme heat stress			>3.5	Very hot	Above 41 °C	Extreme heat stress
+38 to +46 °C	Very strong heat stress	3	Hot	2.5 to 3.5	Hot	35 to 41 °C	Strong heat stress
+32 to +38 °C	Strong heat stress	2	Warm	1.5 to 2.5	Warm	29 to 35 °C	Moderate heat stress
+26 to +32 °C	Moderate heat stress	1	Slightly warm	0.5 to 1.5	Slightly warm	23 to 29 °C	Slight heat stress
+9 to +26 °C	No thermal stress	0	Neutral	−0.5 to 0.5	Neutral	18 to 23 °C	No thermal stress
+9 to 0 °C	Slight cold stress	−1	Slightly cool	−1.5 to −0.5	Slightly cool	13 to 18 °C	Slight cold stress
0 to −13 °C	Moderate cold stress	−2	Cool	−2.5 to −1.5	Cool	8 to 13 °C	Moderate cold stress
−13 to −27 °C	Strong cold stress	−3	Cold	−3.5 to −2.5	Cold	4 to 8 °C	Strong cold stress
−27 to −40 °C	Very strong cold stress			<−3.5	Very cold	Below 4 °C	Extreme cold stress
Below −40 °C	Extreme cold stress						

Just as some of the thermal comfort indexes are more suitable for analysis of thermal environments indoors, such as the PMV, ITS, PT, and OP, some are more accurate when evaluating outdoor thermal environments, such as the UTCI, SET and PET [41]. In a review conducted by [42], wet bulb globe temperature (WBGT), PET and UTCI are the most widely used indexes for outdoor thermal comfort studies, while other studies have shown that that the UTCI provided a better correlation with occupant thermal sensation than the PET, and had the highest correlation with MRT and PMV [26,43].

2.2. Simulation Tools for Outdoor Thermal Comfort Analysis

Different thermal comfort indexes were developed for specific research purposes, hence determining the suitable simulation tools that should be used. Summarised by [44], there are five main types of model which can help to evaluate heat islands: the building energy models, roof energy calculators, canyon and comfort models, ecosystem models, and regional model.

One of the more popular building energy models is EnergyPlus, which is a simulation program for modelling the energy consumption of a building, such as the HVAC system and lighting [45]. EnergyPlus is also capable of integration with other software and models to extend the potential of green roof studies. There is a study which integrates EnergyPlus with the Green Roof Model, known as the EcoRoof model, to allow study of the heat reduction potential of a green roof by modelling the surface energy partitioning and sensible heat fluxes [46]. It is also able to integrate with SketchUP Pro-2019 3D and OpenStudio v3.0.1 software to create 3D models in order to conduct spatial analysis of thermal energy, based on different scenario settings of leaf area index, soil moisture, and plant height [47]. At building scale, EnergyPlus is the popular choice and very accurate in analysing building performance, but at an urban scale analysis might require co-simulation to provide a better model and realistic conditions [48]. For larger scale analysis, the urban energy modelling tool CitySim can be used to analyse the outdoor environmental conditions in the selected urban area based on building materials and vegetation physical properties, such as albedo, conductivity, density, specific heat, LAI, longwave emissivity, etc [49,50]. It can also couple with the Canopy Interface Model to analysis the ground evaporative cooling effects on local UHI intensity [51]. To analysis the urban heat in relation to the unique aerodynamic pattern from the urban canyons formed high-rise building, computational fluid dynamics (CFD) simulation is a suitable approach [52]. ANSYS Fluent (Version 14.5) is a commonly used piece of CFD simulation software, which is capable of handling complex fluid flow and convective heat transfer, by performing turbulence modelling and heat transfer calculations [53]. It allows the study of the interaction between pavement and building albedo and wind velocity on the urban wind-heat environment, which affects UHI intensity [54].

To estimate human comfort, however, software is required to allow inputs of human related parameters, such as metabolism, clothing and activity. RayMan is one of the most commonly used items of software in human comfort analysis due to its ability in calculating radiation on the human body [55]. However, RayMan does not include CFD modelling and does not account for the longwave radiation from the additional reflection of buildings surfaces [56,57]. Another popular outdoor thermal comfort simulation software is ENVI-met. ENVI-met is a microclimate simulation software implemented along with the fundamental law of fluids and thermodynamics [58]. One of the advantages of ENVI-met is the ability to process different settings of materials' albedo, LAI, and evapotranspiration, making it popular for simulating complex urban scenarios with green roofs, green walls, trees, cool pavements, ponds, fountains, etc. [59–65]. Another advantage of ENVI-met is the available thermal comfort indexes output, including PMV, PET, SET, and UTCI [43]. However, as mentioned by [55], although ENVI-met is a very reliable tool to simulate urban planning scenarios, the major challenge is its time-consuming computational requirement. Another limitation is the restriction on spatial and temporal resolution [66].

Grasshopper software with Ladybugs plugin is widely used in thermal comfort studies with parametric design potential [67]. Grasshopper and Ladybugs were developed as a

stand-alone tool and a plug-in for a 3D modelling interface Rhinoceros 7 (sometimes referred to as "Rhino"), which is widely used by design practitioners and students around the world [68]. One big advantage of the integration of Rhinoceros 7 and Grasshopper software is its flexibility in adapting other plugin tools for designers to develop and evaluate the massing for UHI through a single platform [69]. For example, the Urban Weather Generator (UWG) is a code that can be implemented in the Grasshopper Dragonfly tool, which combined four models for urban thermal analysis: (1) rural station model, (2) vertical diffusion model, (3) urban boundary layer model, and (4) urban canyon model [70]. Below, Table 2 provides a summary of the strength and weakness of each simulation software discussed. Among all the microclimate analysis and building energy modelling that has been employed in urban heat studies, the parametric design approach provides a new perspective on building design and urban development.

Table 2. A summary of the advantages and disadvantages of simulation software based on literature review.

Software	Advantages	Disadvantages
EnergyPlus (V 9.3.0)	• Very accurate on simulating building energy performance. • Capable of integrating with other software and modelling to extend analysis aspects. • Free open-source tool • The output files (.eps) are highly compatible with other platforms.	• Requires good understanding on building systems and simulation principle to input detailed data. • Urban scale analysis might require simulation to provide a better model realistic condition.
Rayman 1.2	• Specifically designed to assess human thermal comfort with a wide range of human thermal comfort indices output including: PMV, PET, SET, UTCI, PT, mPET • Relatively easy to use compared to other climate modelling tools in this table. • Free open-source tool • Simple visualization outputs on human comfort.	• Do not include CFD modelling and not account for the longwave radiation from the additional reflection of building surfaces • Limited to thermal comfort simulation as the lack of accuracy for other environmental or energy simulations with complex interactions in the urban environment • Limited integration with other environmental or urban planning tools.
CitySim	• Specifically designed for simulating energy and environmental performance at the urban scale. • Capable of simulating complex energy exchanges with consideration of both shortwave and longwave radiation environment, and allows to fully define building, ground and vegetation entities. • Free open-source tool	• Limited to urban energy simulation only and not suitable other environmental or energy simulations. • Might require specialized training for new users to learn. • Computational requirements are high and time consuming to process complex models.
ANSYS Fluent (V 14.5)	• Well-developed CFD tool with comprehensive modelling capability. • Good reputation in accuracy to process complex fluid flow and convective heat transfer setting.	• Requires significant understanding in CFD which might be complicated for new user. • Computational requirement is high and time consuming to process complex models. • Very expensive on licensing or subscription.
ENVI-met (V 4.1.1)	• Specialized Urban Microclimate Simulation tool which very accurate on outdoor thermal comfort analysis with good range of human thermal comfort indices output includes: PMV, PET, SET, UTCI • Capable of modeling complex interactions between surfaces, vegetation, and atmospheric conditions. • Able to create high quality 3D visualizations	• Might require specialized training for new users to learn. • Computational requirements are high and time consuming to process complex models. • Very expensive on licensing or subscription.
Grasshopper (V.1.0.0007)	• A wide range of plugins is available to allow multiple environmental analysis. With good range of human thermal comfort indices output includes: PMV, PET, SET, UTCI • Highly flexible on modelling and allows for custom parametric design and automation. • Open source integrates with Rhinoceros 3D that able to conduct different scales of analysis	• Require basic understanding of visual programming which might be complicated for new user. • Simulation can be time consuming for very complex models or large datasets. • Although Grasshopper is open source, it requires to purchase the Rhinoceros software to run.

3. Methodology—Parametric Approach to Urban Heat Analysis

In this study, the combination of Rhinoceros Version 7 SR37 (7.37.24107.1500) and Grasshopper (Version 1.0.0007) with Ladybugs plugin was used, as the software allowed flexibility in adapting multiple formats of 3D model and weather data [68,70]. The use

of the parametric design model allows the designer to conduct microclimate analysis in different scales with high flexibility in order to adjust the design parameters, providing better options in the early-stage design. Figure 1 illustrates the workflow of the parametric design framework integrated in this study.

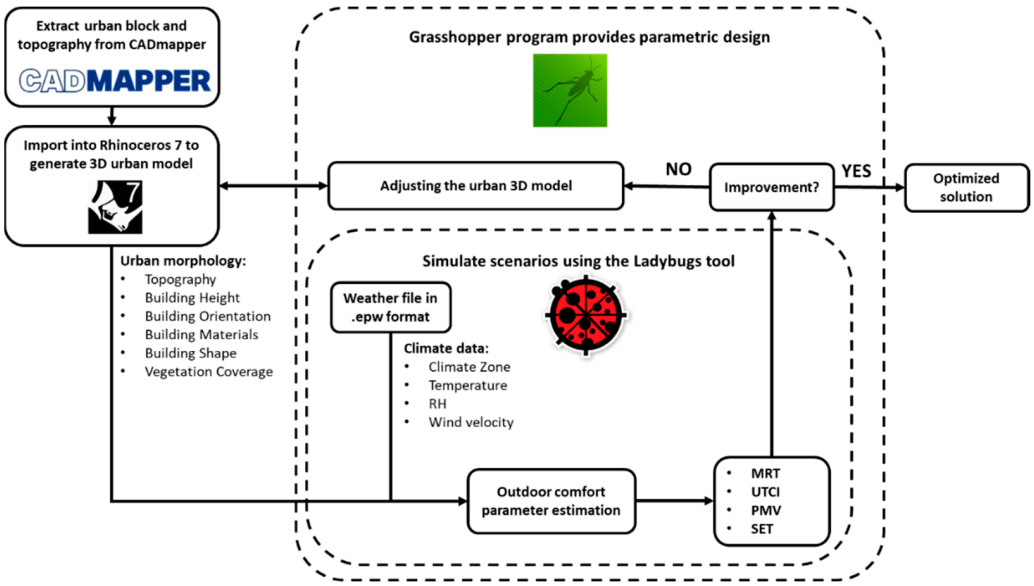

Figure 1. Workflow in the parametric design framework. While Rhinoceros is the main platform to visualise the design outcomes. Components within the dashed line are operated under the Grasshopper programming interface, with Ladybugs as one of the plugin tools from the Grasshopper Program.

The urban heat analysis and outdoor thermal comfort simulation in this study were processed by the combined applications of Rhinoceros 7 software and the Grasshopper program with Ladybugs tools plug-in. Rhinoceros 7 is a computer-aided design application software that allows the modelling of 3D data for early-stage design www.rhino3d.com (accessed on 16 January 2024) [71,72]. The 3D model in Rhinoceros 7 will then be imported into the Grasshopper program, which provides a graphical algorithm editor that synchronizes within the Rhino 3D modelling software www.grasshopper3d.com/ (accessed on 16 January 2024) [73].

3.1. Urban Context and Geometry Input

A 3D urban model of the study location was created by using The CADmapper online tool www.cadmapper.com (accessed on 12 December 2023), which provides free open-source urban model 3D building geometry up to 1-km square in various formats, such as AutoCAD (.dwg), Rhinoceros (.3dm), ArchiCAD (.dxf), Adobe Illustrator (.ai), and SketchUP (.skp). For this study, the 3D model was created in Rhino 5 3dm file type. Within the selected boundary, there is a total of 330 buildings. Only 173 (52%) of the 3D buildings have the building height data from the CADmapper, and the remaining 48% of the buildings were set a false height of 6 m, which required further manual adjustment of the building height in Rhinoceros 7, based on the dataset from the 2020 building footprints captured by the City of Melbourne (data.melbourne.vic.gov.au).

The study area is shown in Figure 2a, located at the Dockland, Melbourne CBD, featuring complex building geometry and landscapes, formed by the Marvel Stadium, Southern Cross Railway Station and the newly built high-rise apartments along Spenser Street. The 3D model created by the CADmapper online tool is shown in Figure 2b. With a diverse range of building types and urban geometry within the Dockland urban area, it offered a unique existing built environment to analyse its urban heat and outdoor thermal comfort.

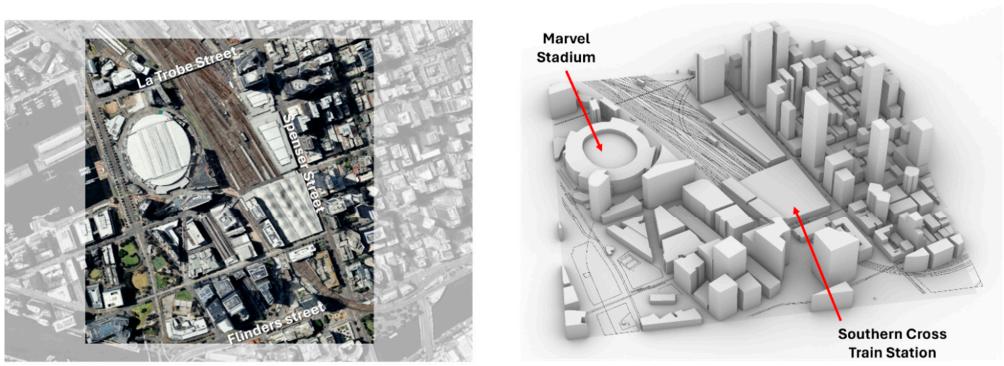

Figure 2. (**a**): 1 km^2 of the selected study area of Dockland, Melbourne CBD; (**b**) the 3D model generated by CADmapper and illustrated in Rhinoceros 7.

3.2. Simulation Process and Workflow in Grasshopper Program with Ladybugs Tools Plugin

The Grasshopper program is an extension with add-on tools of the Rhinoceros 7 computer aided design software. The program uses Python coding language to create an algorithm for conducting numerical analysis and design simulation. The Ladybugs tools plug-in is a set of Python scripts that contain algorithm components specifically designed for meteorology study and thermal comfort analysis based on the 3D model geometry that has been setup in Rhino [56].

The Grasshopper program has simplified the computer programming or script coding by visualizing the Python coding language in different blocks for different command components, which allows the user to drag and connect different components based on the required input and output parameters, then visualize the results on the Rhinoceros 7 interface. The Grasshopper interface and the simulation process of the Ladybugs command components for this study can be divided into a six-step workflow, shown below in Figure 3.

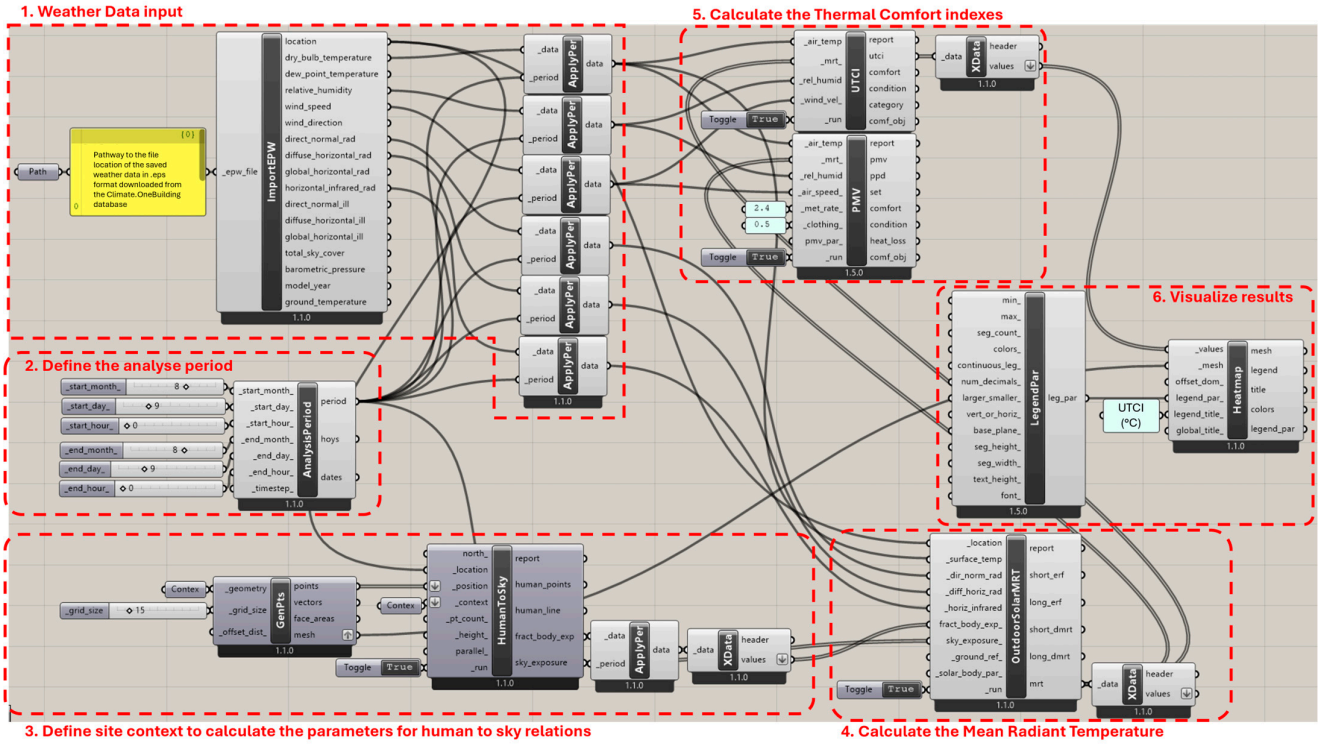

Figure 3. Workflow diagram for the outdoor thermal comfort analysis in Grasshopper with the Ladybugs Tools plugin.

3.2.1. Import the Weather Data Collections

The first step is to import the weather data file to the Ladybugs tools for processing. The weather data were in EnergyPlus Weather Format (epw), which was downloaded from the Climate.OneBuilding database [74]. The source data used the 2007–2021 Typical Meteorological Year (TMYx) dataset, recorded by the weather station RO 948680 located in the Melbourne CBD near Carlton Gardens (S 37°48.45′, E 144°58.20′). The TMYx dataset contains the typical meteorological data derived from hourly values across the years from 2007 to 2021, which means that the monthly data values may come from different years [75]. The Ladybugs weather analysis tools are used to extract the meteorological data collection for microclimate analysis. Some parameters necessary to calculate the outdoor thermal comfort include the dry bulb temperature, Dew point temperature, relative humidity, wind speed, direct normal radiation, diffuse horizontal radiation, and horizontal radiation.

3.2.2. Define the Analysis Period

This component is used to set up the duration of the analysis period and provide the data collections based on the difference between the starting and ending points. A maximum of 8759 values can be generated to represent each hour of a year. This component allows individual analysis of a specific date, week or season, such as an extremely hot day or extremely cold day, to observe the urban heat pattern changes during that day. Note that the duration of the analysis period might also affect the time needed for the computation process, as a longer analysis period requires more time for the computation process when using a larger dataset.

3.2.3. Define Site Context to Calculate the Parameters for Human to Sky Relations

This is the step in which the 3D urban model is integrated into the computation in Grasshopper. The component transfers the 3D objects or mesh into points and a grid in order to process the numerical data collection relevant to the position. All the buildings and ground surface from the urban model are converted into points and a grid with a size of 15, thus a total of 4356 points is created. These points will input to the next component to calculate the parameters for the relationship between human geometry and the sky, based on the position of a human subject and the surrounding geometric contexts using the points created from the 3D objects. There are two outputs that will be used for calculating the outdoor solar MRT: (1) the Fraction of Body Exposure, representing the fraction of the body exposed to direct sunlight, and (2) the Sky Exposure, representing the fraction of the sky vault in the human subject's view.

3.2.4. Calculate the Mean Radiant Temperature

The computation of outdoor solar mean radiant temperature (MRT) in the Ladybugs tool uses the SolarCal model of ASHRAE-55 to estimate the effects of shortwave solar light shining directly onto people, and a simple sky exposure method to determine longwave radiant exchange with the sky.

The component for the MRT calculation requires data collection from the weather file and the outputs from the previous components on human to sky relations. These include the altitude and azimuth of the sun, surface temperature, direct normal solar irradiance, diffuse horizontal solar irradiance, horizontal infrared radiation intensity from the sky, fraction of body exposure, and the sky exposure. Ground reflectance is set to a default of 0.25. Note that, since the surface temperature was unknown, the outdoor dry bulb temperature was used in this study. The result of MRT will be used to estimate the thermal comfort indexes: UTCI, PMV, and SET.

3.2.5. Calculation of the Thermal Comfort Indexes

With the output from the previous components, it is now possible to calculate the thermal comfort indexes, UTCI, PMV, and SET, simultaneously. The UTCI component

requires data collection of ambient air temperature (or dry bulb temperature), MRT, relative humidity, and wind velocity.

The PMV and SET are the outputs from the same command component. The required inputs for calculating the PMV and SET are very similar to the data collection used for calculating the UTCI. The only differences are the PMV and SET required to set values for the metabolic rate (unit in met) and clothing insulation (unit in clo). The typical values for the metabolic rate of a person who is resting seated is 1 met, for standing 1.2 met, and 2.4 met for walking at 1 m/s. The study aims to estimate the outdoor thermal comfort and therefore the value of metabolic rate is set to 2.4 met, which assumes a pedestrian walking speed of 1 m/s. The value of clothing insulation represents the different clothing types and layers a person is wearing. 1 clo means that the person is wearing a three-piece suit, 0.7 clo represents long sleeve shirt and pants, 0.5 clo represent shorts with T-shirt, and 0 clo means no clothing at all. For this study, the value of clothing insulation uses the default 0.7 clo for the whole year analysis, then the value adjusts to 0.5 clo to simulate extreme hot weather, and 1 clo for extreme cold weather.

Note that the lowest air speed input for this UTCI model is recommended at 0.5 m/s, therefore this has been set as the default value for the days with a wind velocity lower than 0.5 m/s. For the PMV or SET, however, the lowest air speed input can be as low as 0.1 m/s, since PMV and SET can also be used for estimating indoor thermal comfort, and 0.1 m/s is a typical indoor air speed induced by HVAC systems.

4. Results and Discussion

After the simulation process for estimating the outdoor thermal comfort indexes by following the workflow in Figure 3, the results can be visualized directly on the 3D model in Rhinoceros using the heatmap component of Ladybugs tool.

Figure 4 displays the heatmaps that illustrate the duration of direct sunlight within the study boundary. The areas with the most direct sunlight are the rooftops without any obstacles, with more than 578 h annually, mainly located to the west of the Southern Cross railway station. The area with the least direct sunlight is that of the narrow laneways across the northeast sector, due to the high-rise buildings blocking most of the sunlight reaching to the ground or lower level. The figure also shows that there is less direct sunlight in areas next to the east facing façade, for example, the open space next to the Marvel Stadium, indicating that sunset might provide the space on the western façade with more direct sunlight during the year. Note that there will never be any direct sunlight on the south facing façade due to the fact that the study site is located in the southern hemisphere.

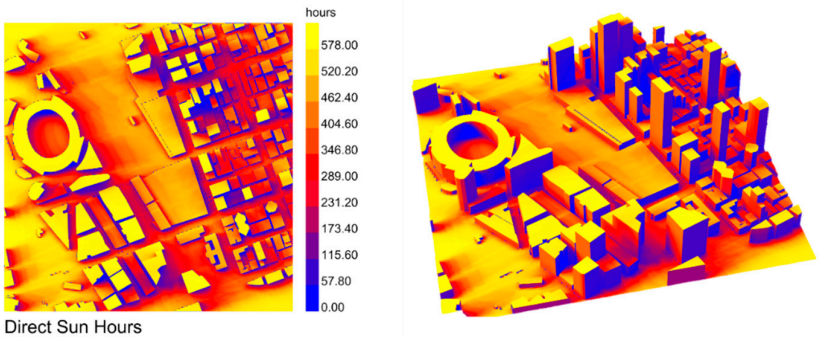

Figure 4. The distribution of annual direct sun hours for the study area.

A similar pattern can be found in Figure 5, illustrating the distribution of the annual incident radiation across the study area. Similarly, the areas with the highest incident radiation values are the rooftop without obstacles, with up to 1834 kWh/m^2. The lowest incident radiation values are mainly distributed in the northeast sector around Spenser Street. Although the distribution pattern is very similar to that of annual direct sunlight, there are two key differences that can be observed. Firstly, unlike direct sunlight, there

is incident radiation recorded on the southern façade of the buildings, and the upper levels have higher values, which might be caused by the reflectance from the surrounding geometry. Secondly, the difference between the western and eastern façade is less significant in comparison to the direct sun hours. These two figures give the idea as to how the sunlight and solar radiation behave at the selected study location, in order to help explain the outdoor thermal comfort results and patterns.

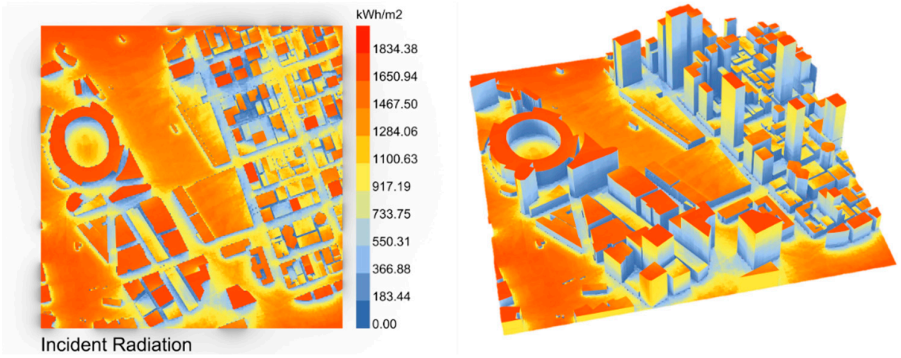

Figure 5. The distribution of annual incident radiation for the study area.

4.1. Outdoor Thermal Comfort Results' Analysis

Figure 6 provides the comparison between the daily average DBT, MRT, UTCI and SET. PMV is not included in this figure because it was not measured in degrees Celsius. The chart in Figure 6a allows identification of the hottest day and the coldest day in the year. Based on the DBT and MRT, the hottest day would be 4 January, with an average daily DBT of 32.68 °C, and average daily MRT of 50.02 °C. However, if using the thermal comfort indexes for determination, 7th February is considered the hottest day during the year, when the daily average of UTCI reaches the highest at 34.96 °C, SET is 30.38 °C and PMV 1.37. On the other hand, the coldest day of the year is easier to determine, as the lowest daily average of DBT is on the 17th June at 6.92 °C, but 9 August has the lowest daily average of MRT (10.2 °C), UTCI (−4.02 °C), SET (6.84 °C), and PMV (−3.79). Knowing which days experienced extreme temperature, the study will then focus on analysing the hourly changes during the day and comparing the results.

To further understand the outdoor thermal comfort in the selected study area, the hourly data were investigated on the hottest day, 7 February, and the coldest day, 9 August. Figure 6b clearly shows that the hottest hour during the hottest day on 7 February is at 3 P.M. according to the thermal comfort indexes, with 55.2 °C UTCI, 39.8 °C SET, and 4.48 PMV. In comparison, the coldest hour during the coldest day is on 9 August at 7 A.M., with −11.0 °C UTCI, 5.02 °C SET, and −3.88 PMV. From Figure 6c, the changes in SET and PMV are not significant, and only UTCI has a larger temperature difference of between −11.0 °C and −0.1 °C.

Based on the hourly outdoor thermal comfort changes during the hottest day and the coldest day, UTCI was selected to conduct the spatial analysis with the 3D urban model, as the UTCI temperature change is more visible then the other two indexes. The illustration in Figure 7 uses the heatmap component in Ladybugs tools to visualize the UTCI distribution of the study area in Dockland, Melbourne. Three different times have been selected as the typical hour during the day: the morning (7 A.M.), the noon (12 P.M.), and the afternoon (3 P.M.), respectively.

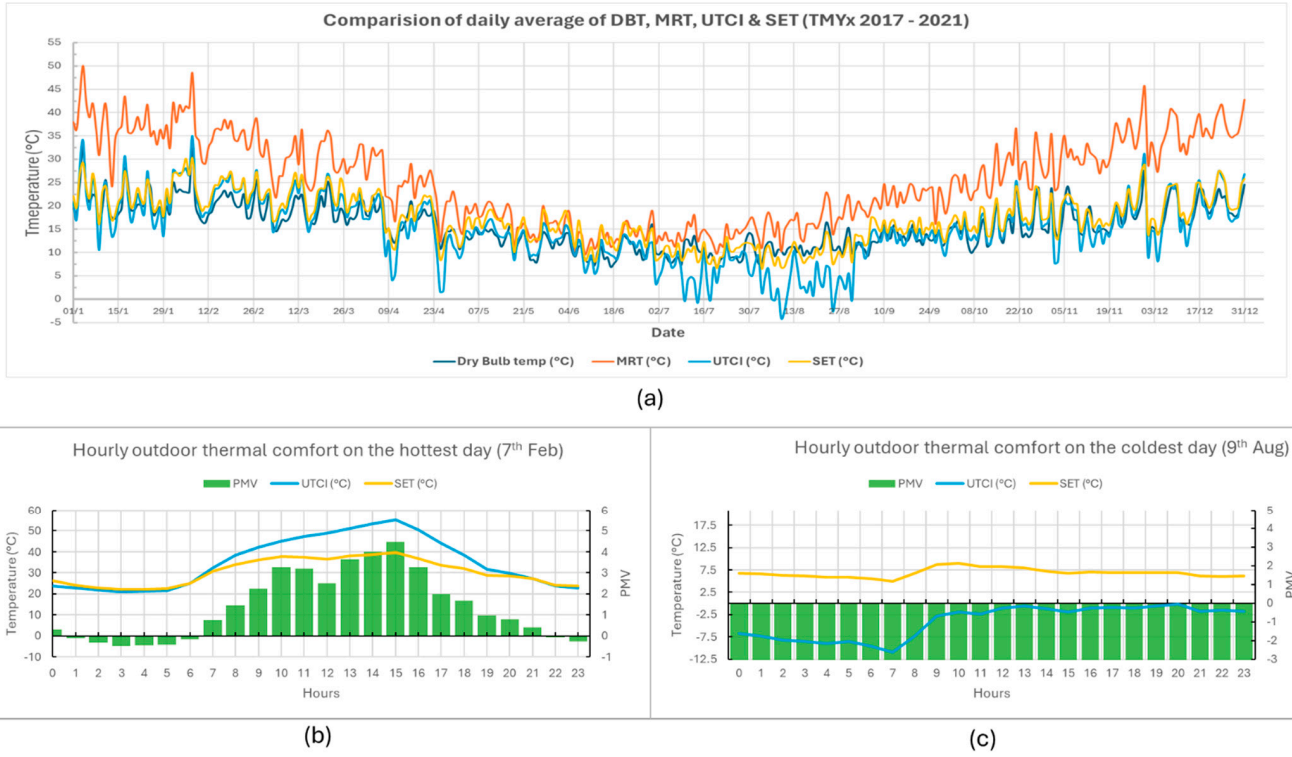

Figure 6. (**a**) Comparison of daily average of DBT, MRT, UTCI and SET using the weather data of TMYx from 2017 to 2021. (**b**) Hourly outdoor thermal comfort of the hottest day on 7 February; (**c**) hourly outdoor thermal comfort of the coldest day on 9 August.

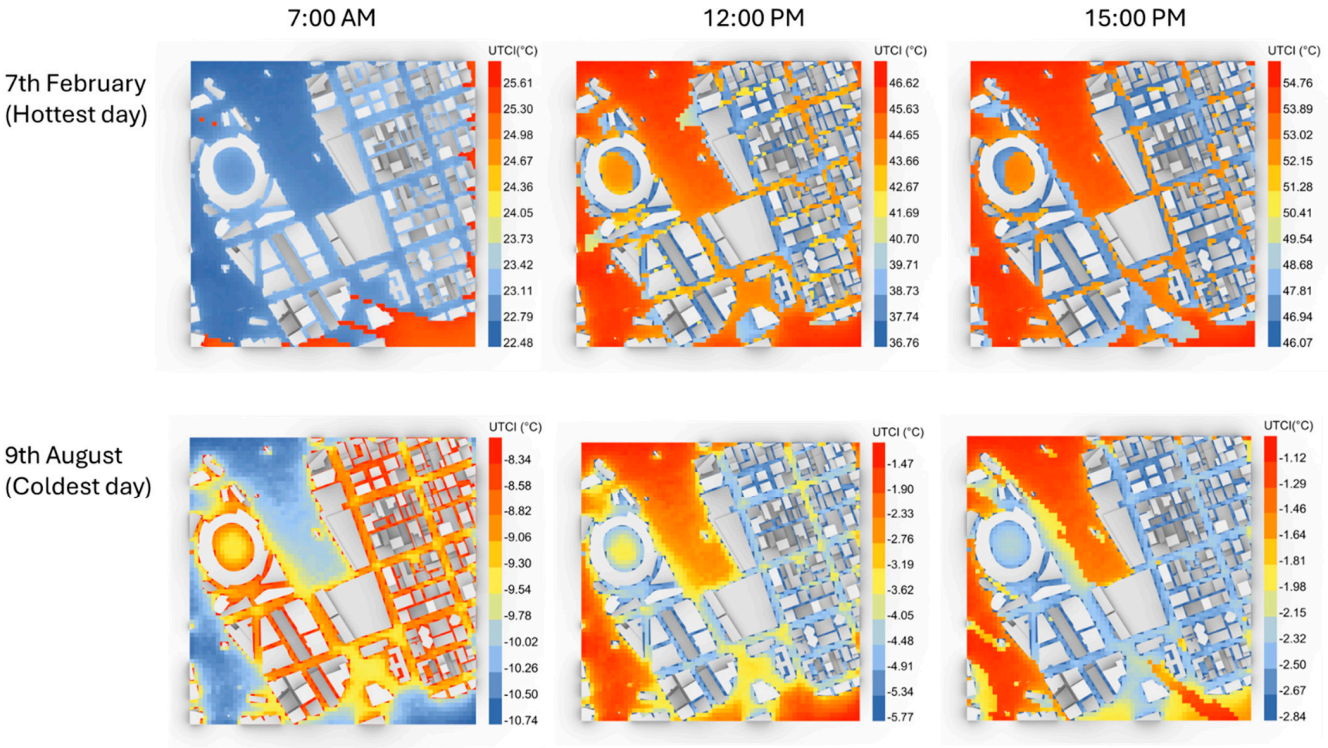

Figure 7. Spatial analysis on the UTCI distribution during the hottest and coldest day in Dockland, Melbourne.

In the morning of the hottest day, the UTCI difference across the study is slight, with the range from 22.48 °C to 25.61 °C, and with higher UTCI values observed in the southeast sector. However, the UTCI rose rapidly at noon, with a range between minimum 36.78 °C and maximum 46.62 °C, where the open space has higher UTCI and the narrow streets between buildings have lower UTCI. From 12 P.M. to 3 P.M., the UTCI continues to increase gradually, and reaches the maximum UTCI of 54.76 °C, with the minimum UTCI at 46.07 °C. The heatmap for the hottest day on the 7 February shows that the UTCI is evenly distributed across the area before sunrise and, once the sun reaches a certain angle, the open space heats up more quickly and more warmly than in the streets between buildings, and this can be 7–10 °C difference, as the buildings' shade reduces the solar radiation reaching the pedestrians at ground level.

For the coldest day on 9 August, the UTCI values across the area during the day are all below 0 °C. The coldest time is 7 AM in the morning before the sun rises, with −10.74 °C in the open space, and the streets surrounded by buildings are slightly warmer, on average 2 °C higher in comparison with the open space. The UTCI temperature increases significantly after sunrise, when the open space heated up to −1.47 °C with almost a 10 °C difference compared to the morning, and the street is slightly cooler in comparison with the open space with −5.77 °C UTCI. The UTCI slightly increases from 12 P.M. to 3 P.M., when the maximum UTCI at −1.12 °C and the minimum UTCI at −2.04 °C. The heatmaps show that the urban heat island event provides a warmer feeling for the pedestrian on the street before sunrise, but the situation alters after sunrise, as the area with direct sunlight has higher UTCI in comparison with the areas without sufficient sunlight.

4.2. Simulations for Various Building Heights

To further investigate the urban heat island effects between high density city areas and the open area within the same microclimate conditions in the study area, the building heights of the 3D urban model are adjusted to create different scenarios for simulation.

The first set of outdoor thermal comfort data used for the building height simulation are from the UTCI data collection for the hottest hours on the 7 February at 15:00 P.M., the building height set to 10 m, 30 m and 50 m on Rhino7 software, respectively (see Figure 8). At 10 m, most of the area appears to have the maximum UTCI of 50.31 °C, the only areas with lower UTCI were adjacent to the building and mainly on the east facing façade, which may have the minimum UTCI of 42.44 °C. A major difference in UTCI distribution can be observed when the building height is adjusted to 30 m, when the maximum UTCI reduced slightly to 50.17 °C, but the minimum UTCI remains at 42.44 °C. While the UTCI range is similar, there are more areas now with lower UTCI compared to the 10 m scenario, with an increased area on the east side of the buildings, and on the streets with north–south orientation. When the building height increases to 50 m, the maximum UTCI is further reduced to 50.05 °C, with the same value for the minimum UTCI, and the area with the lower UTCI also increased, mainly on the east side of the building and the streets surrounded by buildings.

The second set of heatmaps shown in Figure 9 display the UTCI distribution using the data collection from the coldest hours on 9 August at 07:00 A.M., with the same variation in building height scenarios. In the first design scenario with all the buildings set to 10 m tall, the majority of areas experienced moderate cold stress; the middle of the open space showed the minimum UTCI of −11.0 °C, while the maximum UTCI is −8.34 °C on areas closest to buildings. The UTCI distribution changes drastically when the building heights are modified to 30 m, and the majority of the streets surrounded by buildings showed an overall increase in UTCI, and the minimum UTCI had a slight reduction from −10.99 °C to −10.88 °C, while the maximum UTCI remains −8.34 °C. A similar pattern occurs when the building height of the model increases to 50 m, with a further reduction in the minimum UTCI to −10.79 °C with the same maximum UTCI.

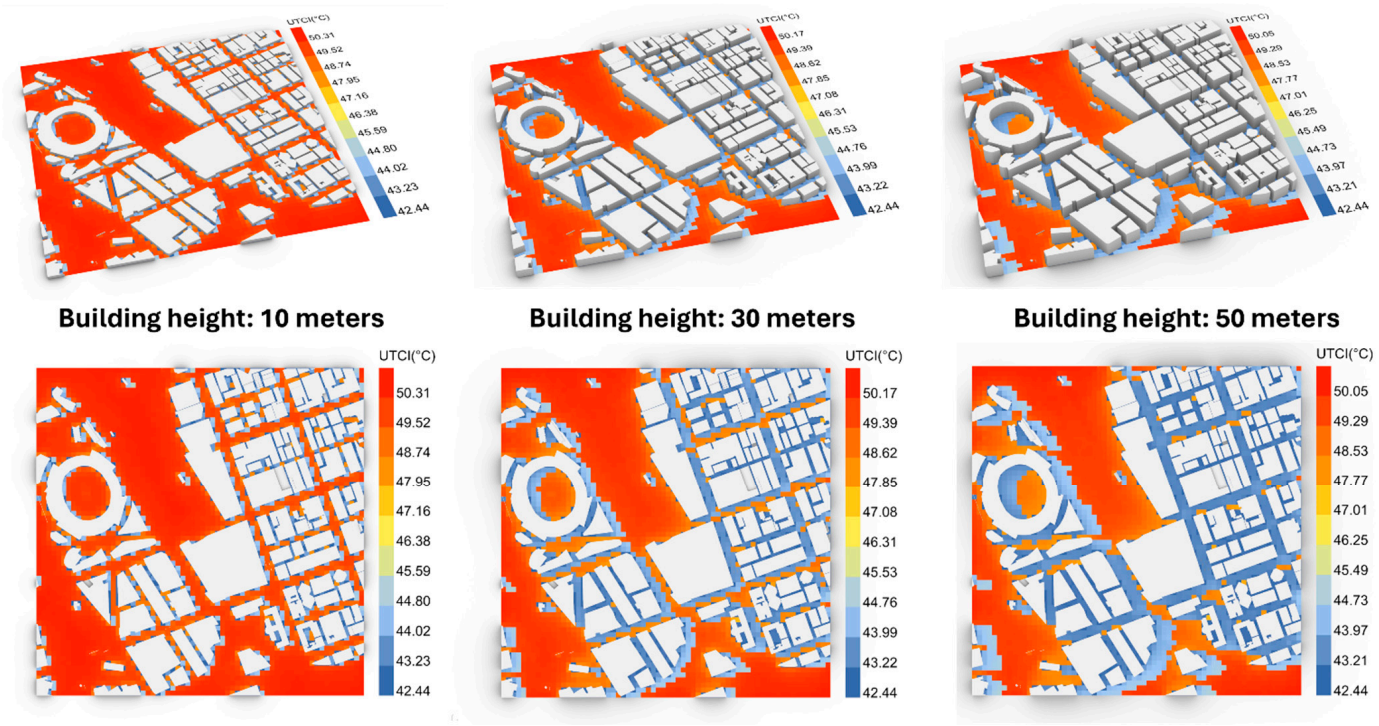

Figure 8. UTCI distribution at the hottest hour with different building height settings of 10 m, 30 m, and 50 m.

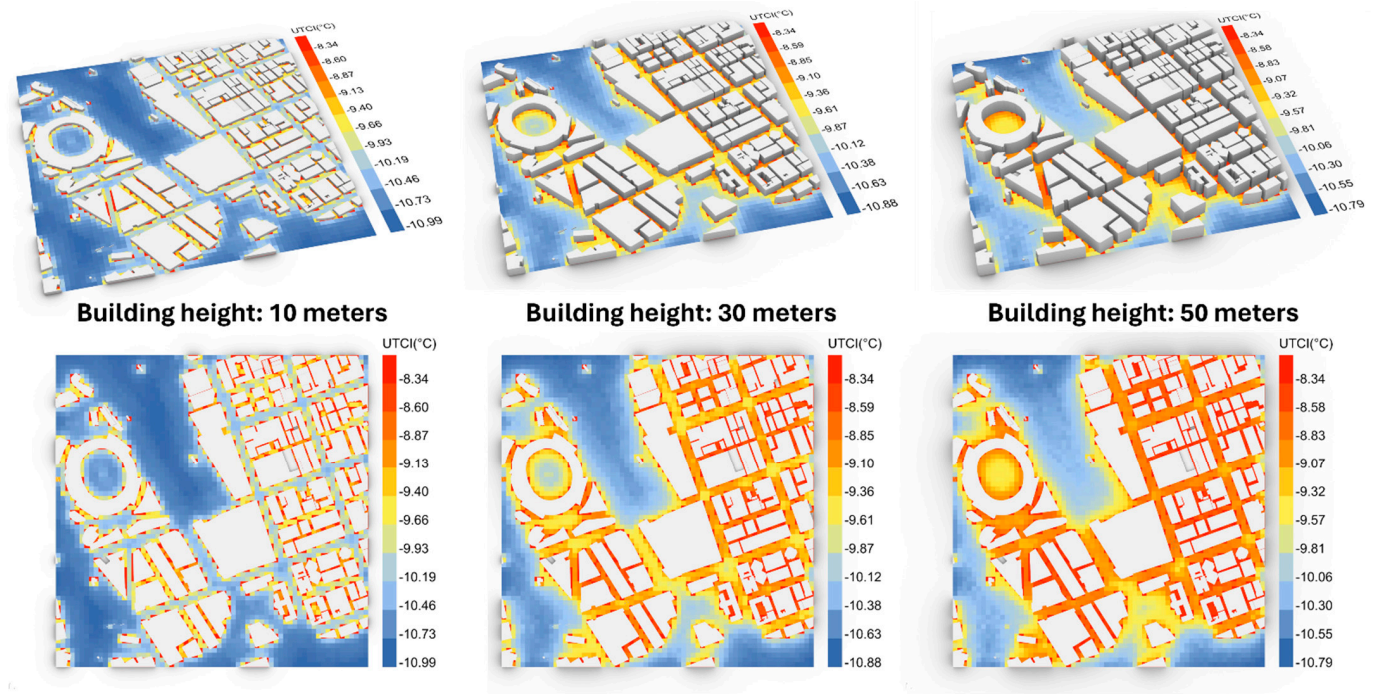

Figure 9. UTCI distribution at the coldest hour with different building height settings of 10 m, 30 m, and 50 m.

4.3. Discussion

The simulation results provide a better understanding of different scenarios for outdoor thermal comfort and microclimate patterns associated with the existing built environment under typical Melbourne climate characteristics. The result shows that the MRT has strong correlation with UTCI when compared with the correlation between PMV and

SET, which means that UTCI is the more accurate index when it comes to outdoor thermal comfort analysis at neighborhood scale. The results of the outdoor thermal comfort simulation on the hottest day and coldest day show that the existing urban design in the Melbourne CBD provides better thermal comfort performance during wintertime, as the city area protects the pedestrian from strong winds. This result matches the simulation study carried out by Hong and Lin [76], which shows that the building form of courtyard dwelling is effective in protecting the central site from wind in cold winters.

Overall, the heatmaps generated based on the various building height scenarios show that solar radiation plays an important role in outdoor thermal comfort in the existing built environment. The simulation results show that the UTCI distribution changed significantly after sunrise. During the summertime, the increase in building heights helps to reduce the maximum and average UTCI, but has less impact on the minimum UTCI value, due to the shading effect from the tall buildings. This result is similar to the study conducted by Mohamed and Neveen [77], who found that shading helps to cause a reduction of 2.3C in air temperature under the best case scenario of street canopy design. Similar results were observed in the winter analysis where the minimal UTCI value would change with building height, while the maximum UTCI value remains the same.

5. Conclusions

With the increasing risk urban heat poses to human health and well-being, many outdoor thermal comfort studies have been conducted using different thermal comfort indexes and methodologies. Simulations using parametric design software were integrated in this study to provide a better understanding of the impact of human outdoor thermal comfort in relation to the interactions between the existing built environment and microclimate pattern. A neighbourhood scale city block 3D model was created in Rhinoceros 7 software to represent the urban area of Dockland, Melbourne CBD. The outdoor thermal comfort analysis was based on the 2017–2021 TMYx historical meteorological dataset using Ladybug plugin on the Grasshopper program, to create various scenarios under different building settings for the selected study area.

Comparing the thermal comfort indexes during the hottest and coldest day shows that the UTCI and SET fluctuation in summer is large, with 20 to 40 °C difference during the day; meanwhile, the fluctuation in winter only leads to a 7.5 °C difference, due to the fact that the solar radiation difference on the hottest day is more significant than on the coldest day. This indicates that solar radiation seems to be the key factor and has a dominant impact on outdoor thermal comfort during the summer period or extreme hot weather, with less influence in winter or extreme cold weather in comparison with other factors, such as wind speed and direction, which might be the dominant factors during cold periods. The maps also show that open space surrounded by structures, such as a field within a stadium or a courtyard space between buildings, has better thermal comfort compared to open space without any obstacles, such as railways and the multi-lane driveway. Therefore, it will be beneficial to implement urban ecosystem services, such as increased tree canopy and vegetation coverage, to reduce the heat gain from solar radiation during hot summers.

In built environments, where ecosystem services are compromised by buildings, thermal comfort can be negatively affected. This is because tall buildings can diminish the ability of vegetation to provide cooling services, which play a crucial role in regulating urban temperatures. The results from the six scenarios demonstrated that change in building height significantly impacts the surrounding outdoor environment. The low-rise scenarios with all buildings capped at 10 m resulted in poor thermal comfort across the city, particularly in open spaces. While thermal comfort improves in the street canyons as building height increases, there were negligible changes in the open spaces. These simulation scenarios show that the potential of urban geometry manipulation can be successfully implemented with careful planning of building height and location that maximises the shading effect during summer, but retains an urban heat island effect during wintertime.

It is recommended to further investigate building materials, vegetation coverage, and presentation of water bodes to evaluate the actual impacts of the shading effect, wind patterns, and evapotranspiration impacts on pedestrians between the summer and winter periods. Moreover, although the TMYx meteorological data capably demonstrate the most typical weather conditions for each month to simulate specific scenarios in the past, they do not provide for most of the current weather conditions in comparison with studies using real-time data, nor do they provide any predictions with regards to climate change patterns; therefore, for urban planners and building designers with aims to create a built environment that will last for decades, is recommended to develop different climate change scenarios to provide better estimation of the urban thermal pattern in future and in regard to the rapid urban development in the area.

Author Contributions: Conceptualization, C.Y.W., M.A.U.R.T. and N.M.; Data curation, C.Y.W. and M.A.U.R.T.; Formal analysis, C.Y.W. and N.M.; Investigation, M.A.U.R.T. and C.Y.W.; Methodology, C.Y.W. and N.M.; Software, C.Y.W., M.A.U.R.T. and H.-W.C.; Supervision, M.A.U.R.T., H.-W.C. and N.M.; Validation, H.-W.C. and N.M.; Visualization, C.Y.W., M.A.U.R.T. and E.J.; Writing—original draft, M.A.U.R.T. and C.Y.W.; Writing—review and editing, H.-W.C., E.J. and N.M. All authors have read and agreed to the published version of the manuscript.

Funding: This research received no external funding.

Data Availability Statement: The raw data supporting the conclusions of this article will be made available by the authors on request.

Conflicts of Interest: The authors declare no conflicts of interest.

References

1. Oke, T.R. The energetic basis of the urban heat island. *Q. J. R. Meteorol. Soc.* **1982**, *108*, 1–24. [CrossRef]
2. Pianella, A.; Aye, L.; Chen, Z.; Williams, N.S.G. Effects of substrate depth and native plants on green roof thermal performance in South-East Australia. *IOP Conf. Ser. Earth Environ. Sci.* **2020**, *588*, 22057. [CrossRef]
3. Wang, Y.; Wang, J.; Zhang, H.; Janechek, N.; Wang, Y.; Zhou, M.; Shen, P.; Tan, J.; He, Q.; Cheng, T.; et al. Impact of land use change on the urban-rural temperature disparity in Eastern China. *Atmos. Environ.* **2023**, *308*, 119850. [CrossRef]
4. Li, J.; Donn, M.; Thomas, G. The influence of urban microclimate vertical variations on the building performance of a high-rise office building at different floors. *IOP Conf. Ser. Mater. Sci. Eng.* **2019**, *609*, 32027. [CrossRef]
5. Heaviside, C.; Macintyre, H.; Vardoulakis, S. The Urban Heat Island: Implications for Health in a Changing Environment. *Curr. Environ. Health Rep.* **2017**, *4*, 296–305. [CrossRef] [PubMed]
6. Ngarambe, J.; Santamouris, M.; Yun, G.Y. The Impact of Urban Warming on the Mortality of Vulnerable Populations in Seoul. *Sustainability* **2022**, *14*, 13452. [CrossRef]
7. IEA. Renewables 2019: Analysis and Forecast to 2024, Paris. 2019. Available online: https://iea.blob.core.windows.net/assets/a846e5cf-ca7d-4a1f-a81b-ba1499f2cc07/Renewables_2019.pdf (accessed on 22 October 2023).
8. Milne, G.; Reardon, C.; Ryan, P.; Pavia, M.; Wyndham, J. Energy—Heating and Cooling. In *Your Home: Australia's Guide to Environmentally Sustainable Homes*, 6th ed.; Department of Climate Change, Energy, the Environment and Water: Canberra, Australia, 2023.
9. DCCEEW. Australian Energy Update 2023, Canberra. 2023. Available online: https://www.energy.gov.au/sites/default/files/Australian%20Energy%20Update%202023_0.pdf (accessed on 10 November 2023).
10. Ritchie, H.; Rosado, P.; Roser, M. Emissions by Sector: Where Do Greenhouse Gases Come from? Our World in Data. 2020. Available online: https://ourworldindata.org/emissions-by-sector (accessed on 19 October 2023).
11. Emmanuel, R. *An Urban Approach to Climate Sensitive Design: Strategies for the Tropics*; CRC Press LLC: Oxford, UK, 2005; ISBN 9780203414644.
12. Jamei, E.; Ossen, D.R.; Seyedmahmoudian, M.; Sandanayake, M.; Stojcevski, A.; Horan, B. Urban design parameters for heat mitigation in tropics. *Renew. Sustain. Energy Rev.* **2020**, *134*, 110362. [CrossRef]
13. Wai, C.Y.; Tariq, M.A.U.R.; Muttil, N. A Systematic Review on the Existing Research, Practices, and Prospects Regarding Urban Green Infrastructure for Thermal Comfort in a High-Density Urban Context. *Water* **2022**, *14*, 2496. [CrossRef]
14. Kim, S.W.; Brown, R.D. Urban heat island (UHI) intensity and magnitude estimations: A systematic literature review. *Sci. Total Environ.* **2021**, *779*, 146389. [CrossRef]
15. Ma, R.; Ren, B.; Zhao, D.; Chen, J.; Lu, Y. Modeling urban energy dynamics under clustered urban heat island effect with local-weather extended distributed adjacency blocks. *Sustain. Cities Soc.* **2020**, *56*, 102099. [CrossRef]
16. Smalls-Mantey, L.; Montalto, F. The seasonal microclimate trends of a large scale extensive green roof. *Build. Environ.* **2021**, *197*, 107792. [CrossRef]

17. Wai, C.Y.; Muttil, N.; Tariq, M.A.U.R.; Paresi, P.; Nnachi, R.C.; Ng, A.W.M. Investigating the Relationship between Human Activity and the Urban Heat Island Effect in Melbourne and Four Other International Cities Impacted by COVID-19. *Sustainability* **2022**, *14*, 378. [CrossRef]
18. Ahmed, A.Q.; Ossen, D.R.; Jamei, E.; Manaf, N.A.; Said, I.; Ahmad, M.H. Urban surface temperature behaviour and heat island effect in a tropical planned city. *Theor. Appl. Climatol.* **2015**, *119*, 493–514. [CrossRef]
19. Pritipadmaja; Garg, R.D.; Sharma, A.K. Assessing the Cooling Effect of Blue-Green Spaces: Implications for Urban Heat Island Mitigation. *Water* **2023**, *15*, 2983. [CrossRef]
20. Mendez-Astudillo, J.; Lau, L.; Tang, Y.-T.; Moore, T. Determination of Air Urban Heat Island Parameters with High-Precision GPS Data. *Atmosphere* **2022**, *13*, 417. [CrossRef]
21. Rajapaksha, S.; Nnachi, R.C.; Tariq, M.A.; Ng, A.W.M.; Abid, M.M.; Sidiqui, P.; Rais, M.F.; Aamir, E.; Herrera Diaz, L.; Kimiaei, S.; et al. An Estimation of the Anthropogenic Heat Emissions in Darwin City Using Urban Microclimate Simulations. *Sustainability* **2022**, *14*, 5218. [CrossRef]
22. Padmanaban, R.; Bhowmik, A.K.; Cabral, P. Satellite image fusion to detect changing surface permeability and emerging urban heat islands in a fast-growing city. *PLoS ONE* **2019**, *14*, e0208949. [CrossRef] [PubMed]
23. Sidiqui, P.; Tariq, M.A.; Ng, A.W.M. An Investigation to Identify the Effectiveness of Socioeconomic, Demographic, and Buildings’ Characteristics on Surface Urban Heat Island Patterns. *Sustainability* **2022**, *14*, 2777. [CrossRef]
24. Li, D.; Liao, W.; Rigden, A.J.; Liu, X.; Wang, D.; Malyshev, S.; Shevliakova, E. Urban heat island: Aerodynamics or imperviousness? *Sci. Adv.* **2023**, *5*, eaau4299. [CrossRef]
25. Kong, J.; Zhao, Y.; Carmeliet, J.; Lei, C. Urban Heat Island and Its Interaction with Heatwaves: A Review of Studies on Mesoscale. *Sustainability* **2021**, *13*, 10923. [CrossRef]
26. Xue, J.; Hu, X.; Sani, S.N.; Wu, Y.; Li, X.; Chai, L.; Lai, D. Outdoor Thermal Comfort at a University Campus: Studies from Personal and Long-Term Thermal History Perspectives. *Sustainability* **2020**, *12*, 9284. [CrossRef]
27. Pantavou, K.; Kotroni, V.; Lagouvardos, K. Thermal environment and indices: An analysis for effectiveness in operational weather applications in a Mediterranean city (Athens, Greece). *Int. J. Biometeorol.* **2024**, *68*, 79–87. [CrossRef] [PubMed]
28. Streinu-Cercel, A.; Costoiu, S.; Mârza, M.; Streinu-Cercel, A.; Mârza, M. Models for the indices of thermal comfort. *J. Med. Life* **2008**, *1*, 148–156. [PubMed]
29. Laouadi, A. A New General Formulation for the PMV Thermal Comfort Index. *Buildings* **2022**, *12*, 1572. [CrossRef]
30. Zhao, Q.; Lian, Z.; Lai, D. Thermal comfort models and their developments: A review. *Energy Built Environ.* **2021**, *2*, 21–33. [CrossRef]
31. Fanger, P.O. *Thermal Comfort*; Danish Technical Press: Copenhagen, Denmark, 1970.
32. *ANSI/ASHRAE Standard 55*; Thermal Environmental Conditions for Human Occupancy. ASHRAE: Peachtree Corners, GA, USA, 2023.
33. Kontogianni, E.; Giannakis, G.; Kontes, G.; Rovas, D. Comparing the impact of different thermal comfort constraints on a model-assisted control design process. In Proceedings of the CLIMA 2013, Prague, Czech Republic, 16–19 June 2013; Kabelo, K., Ed.; UCL Discovery: London, UK, 2013; pp. 4193–4203.
34. Yang, L.; Yan, H.; Lam, J.C. Thermal comfort and building energy consumption implications—A review. *Appl. Energy* **2014**, *115*, 164–173. [CrossRef]
35. Fiala, D.; Havenith, G.; Bröde, P.; Kampmann, B.; Jendritzky, G. UTCI-Fiala multi-node model of human heat transfer and temperature regulation. *Int. J. Biometeorol.* **2012**, *56*, 429–441. [CrossRef] [PubMed]
36. Brode, P.; Blazejczyk, K.; Fiala, D.; Havenith, G.; Holmer, I.; Jendritzky, G.; Kuklane, K.; Kampmann, B. The Universal Thermal Climate Index UTCI Compared to Ergonomics Standards for Assessing the Thermal Environment. *Ind. Health* **2013**, *51*, 16–24. [CrossRef] [PubMed]
37. Huang, Q.; Meng, X.; Yang, X.; Jin, L.; Liu, X.; Hu, W. The Ecological City: Considering Outdoor Thermal Environment. *Energy Procedia* **2016**, *104*, 177–182. [CrossRef]
38. Höppe, P. The physiological equivalent temperature—A universal index for the biometeorological assessment of the thermal environment. *Int. J. Biometeorol.* **1999**, *43*, 71–75. [CrossRef]
39. Matzarakis, A.; Amelung, B. Physiological Equivalent Temperature as Indicator for Impacts of Climate Change on Thermal Comfort of Humans. In *Seasonal Forecasts, Climatic Change and Human Health: Health and Climate*; Thomson, M.C., Garcia-Herrera, R., Beniston, M., Eds.; Springer: Dordrecht, The Netherlands, 2008; pp. 161–172, ISBN 978-1-4020-6877-5.
40. Matzarakis, A.; Mayer, H. Heat stress in Greece. *Int. J. Biometeorol.* **1997**, *41*, 34–39. [CrossRef] [PubMed]
41. Li, H. Chapter 13—Impacts of Pavement Strategies on Human Thermal Comfort. In *Pavement Materials for Heat Island Mitigatio*; Li, H., Ed.; Butterworth-Heinemann: Boston, UK, 2016; pp. 281–306, ISBN 978-0-12-803476-7.
42. Ren, J.; Shi, K.; Li, Z.; Kong, X.; Zhou, H. A Review on the Impacts of Urban Heat Islands on Outdoor Thermal Comfort. *Buildings* **2023**, *13*, 1368. [CrossRef]
43. Mahdavinejad, M.; Shaeri, J.; Nezami, A.; Goharian, A. Comparing universal thermal climate index (UTCI) with selected thermal indices to evaluate outdoor thermal comfort in traditional courtyards with BWh climate. *Urban Clim.* **2024**, *54*, 101839. [CrossRef]
44. Gartland, L. Measuring and modelling heat islands. In *Heat Islands: Understanding and Mitigating Heat in Urban Areas*; Earthscan: London, UK, 2008; pp. 27–41, ISBN 9781844072507.
45. Ruz, M.L.; Garrido, J.; Vázquez, F. Educational tool for the learning of thermal comfort control based on PMV-PPD indices. *Comput. Appl. Eng. Educ.* **2018**, *26*, 906–917. [CrossRef]

46. Heusinger, J.; Sailor, D.J.; Weber, S. Modeling the reduction of urban excess heat by green roofs with respect to different irrigation scenarios. *Build. Environ.* **2018**, *131*, 174–183. [CrossRef]
47. Abuseif, M.; Jamei, E.; Chau, H.-W. Simulation-based study on the role of green roof settings on energy demand reduction in seven Australian climate zones. *Energy Build.* **2023**, *286*, 112938. [CrossRef]
48. Miller, C.; Thomas, D.; Kämpf, J.; Schlueter, A. Urban and building multiscale co-simulation: Case study implementations on two university campuses. *J. Build. Perform. Simul.* **2018**, *11*, 309–321. [CrossRef]
49. Andreucci, M.B.; Cupelloni, L.; Delli Paoli, M.; Coccolo, S. Restorative design of urban brownfields, an interdisciplinary approach interconnecting nature-based solutions, heritage requalification and human wellbeing. A case study in Rome. In Proceedings of the Building Simulation, Rome, Italy, 2–4 September 2019.
50. Coccolo, S.; Pearlmutter, D.; Kaempf, J.; Scartezzini, J.-L. Thermal Comfort Maps to estimate the impact of urban greening on the outdoor human comfort. *Urban For. Urban Green.* **2018**, *35*, 91–105. [CrossRef]
51. Mauree, D.; Coccolo, S.; Scartezzini, J.-L. Impact of evapotranspiration on the local microclimate. *J. Phys. Conf. Ser.* **2019**, *1343*, 12009. [CrossRef]
52. Zhang, K.; Chen, G.; Wang, X.; Liu, S.; Mak, C.M.; Fan, Y.; Hang, J. Numerical evaluations of urban design technique to reduce vehicular personal intake fraction in deep street canyons. *Sci. Total Environ.* **2019**, *653*, 968–994. [CrossRef]
53. Nazarian, N.; Kleissl, J. CFD simulation of an idealized urban environment: Thermal effects of geometrical characteristics and surface materials. *Urban Clim.* **2015**, *12*, 141–159. [CrossRef]
54. Wang, J.; Chen, J.; Wu, J.; Zhou, Z. Investigation into the effect of pavement albedo and environmental factors on urban heat island effect using CFD simulation. In *Functional Pavements*; CRC Press: Boca Raton, FL, USA, 2020; pp. 389–395, ISBN 1003156223.
55. Balany, F.; Ng, A.W.M.; Muttil, N.; Muthukumaran, S.; Wong, M.S. Green infrastructure as an urban heat island mitigation strategy—A review. *Water* **2020**, *12*, 3577. [CrossRef]
56. Aghamolaei, R.; Fallahpour, M.; Mirzaei, P.A. Tempo-spatial thermal comfort analysis of urban heat island with coupling of CFD and building energy simulation. *Energy Build.* **2021**, *251*, 111317. [CrossRef]
57. Matzarakis, A.; Rutz, F.; Mayer, H. Modelling radiation fluxes in simple and complex environments: Basics of the RayMan model. *Int. J. Biometeorol.* **2010**, *54*, 131–139. [CrossRef] [PubMed]
58. López-Cabeza, V.P.; Galán-Marín, C.; Rivera-Gómez, C.; Roa-Fernández, J. Courtyard microclimate ENVI-met outputs deviation from the experimental data. *Build. Environ.* **2018**, *144*, 129–141. [CrossRef]
59. Balany, F.; Muttil, N.; Muthukumaran, S.; Wong, M.S.; Ng, A.W.M. Studying the Effect of Blue-Green Infrastructure on Microclimate and Human Thermal Comfort in Melbourne's Central Business District. *Sustainability* **2022**, *14*, 9057. [CrossRef]
60. Razzaghmanesh, M.; Beecham, S.; Salemi, T. The role of green roofs in mitigating Urban Heat Island effects in the metropolitan area of Adelaide, South Australia. *Urban For. Urban Green.* **2016**, *15*, 89–102. [CrossRef]
61. Fahmy, M.; Ibrahim, Y.; Hanafi, E.; Barakat, M. Would LEED-UHI greenery and high albedo strategies mitigate climate change at neighborhood scale in Cairo, Egypt? *Build. Simul.* **2018**, *11*, 1273–1288. [CrossRef]
62. Pigliautile, I.; Chàfer, M.; Pisello, A.L.; Pérez, G.; Cabeza, L.F. Inter-building assessment of urban heat island mitigation strategies: Field tests and numerical modelling in a simplified-geometry experimental set-up. *Renew. Energy* **2020**, *147*, 1663–1675. [CrossRef]
63. Battista, G.; de Lieto Vollaro, E.; de Lieto Vollaro, R. How Cool Pavements and Green Roof Affect Building Energy Performances. *Heat Transf. Eng.* **2022**, *43*, 326–336. [CrossRef]
64. Herath, H.M.P.I.K.; Halwatura, R.U.; Jayasinghe, G.Y. Evaluation of green infrastructure effects on tropical Sri Lankan urban context as an urban heat island adaptation strategy. *Urban For. Urban Green.* **2018**, *29*, 212–222. [CrossRef]
65. Wang, Y.; Ni, Z.; Hu, M.; Chen, S.; Xia, B. A practical approach of urban green infrastructure planning to mitigate urban overheating: A case study of Guangzhou. *J. Clean. Prod.* **2021**, *287*, 124995. [CrossRef]
66. Zölch, T.; Maderspacher, J.; Wamsler, C.; Pauleit, S. Using green infrastructure for urban climate-proofing: An evaluation of heat mitigation measures at the micro-scale. *Urban For. Urban Green.* **2016**, *20*, 305–316. [CrossRef]
67. Liu, K.; Xu, X.; Huang, W.; Zhang, R.; Kong, L.; Wang, X. A multi-objective optimization framework for designing urban block forms considering daylight, energy consumption, and photovoltaic energy potential. *Build. Environ.* **2023**, *242*, 110585. [CrossRef]
68. de Sousa Freitas, J.; Cronemberger, J.; Soares, R.M.; Amorim, C.N.D. Modeling and assessing BIPV envelopes using parametric Rhinoceros plugins Grasshopper and Ladybug. *Renew. Energy* **2020**, *160*, 1468–1479. [CrossRef]
69. Nakano, A.; Bueno, B.; Norford, L.; Reinhart, C.F. Urban Weather Generator—A novel workflow for integrating urban heat island effect within urban design process. In Proceedings of the 14th Conference of International Building Performance Simulation Association, BS2015, Hyderabad, India, 7–9 December 2015.
70. Dardir, M.; Berardi, U. Development of microclimate modeling for enhancing neighborhood thermal performance through urban greenery cover. *Energy Build.* **2021**, *252*, 111428. [CrossRef]
71. Lobaccaro, G.; Croce, S.; Vettorato, D.; Carlucci, S. A holistic approach to assess the exploitation of renewable energy sources for design interventions in the early design phases. *Energy Build.* **2018**, *175*, 235–256. [CrossRef]
72. Hu, Y.; Peng, Y.; Gao, Z.; Xu, F. Application of CFD plug-ins integrated into urban and building design platforms for performance simulations: A literature review. *Front. Archit. Res.* **2022**, *12*, 148–174. [CrossRef]
73. Vuckovic, M.; Loibl, W.; Tötzer, T.; Stollnberger, R. Potential of Urban Densification to Mitigate the Effects of Heat Island in Vienna, Austria. *Environments* **2019**, *6*, 82. [CrossRef]

74. Climate One Building. Repository of Free Climate Data for Building Performance Simulation. 2023. Available online: https://climate.onebuilding.org/ (accessed on 7 September 2023).
75. Renné, D.S. 2—Resource assessment and site selection for solar heating and cooling systems. In *Advances in Solar Heating and Cooling*; Wang, R.Z., Ge, T.S., Eds.; Woodhead Publishing: Sawston, UK, 2016; pp. 13–41, ISBN 978-0-08-100301-5.
76. Hong, B.; Lin, B. Numerical study of the influences of different patterns of the building and green space on micro-scale outdoor thermal comfort and indoor natural ventilation. *Build. Simul.* **2014**, *7*, 525–536. [CrossRef]
77. Elnabawi, M.H.; Hamza, N. Outdoor Thermal Comfort: Coupling Microclimatic Parameters with Subjective Thermal Assessment to Design Urban Performative Spaces. *Buildings* **2020**, *10*, 238. [CrossRef]